iScience

CellPress
OPEN ACCESS

Article

Crabtree effect in kidney proximal tubule cells via late-stage glycolytic intermediates

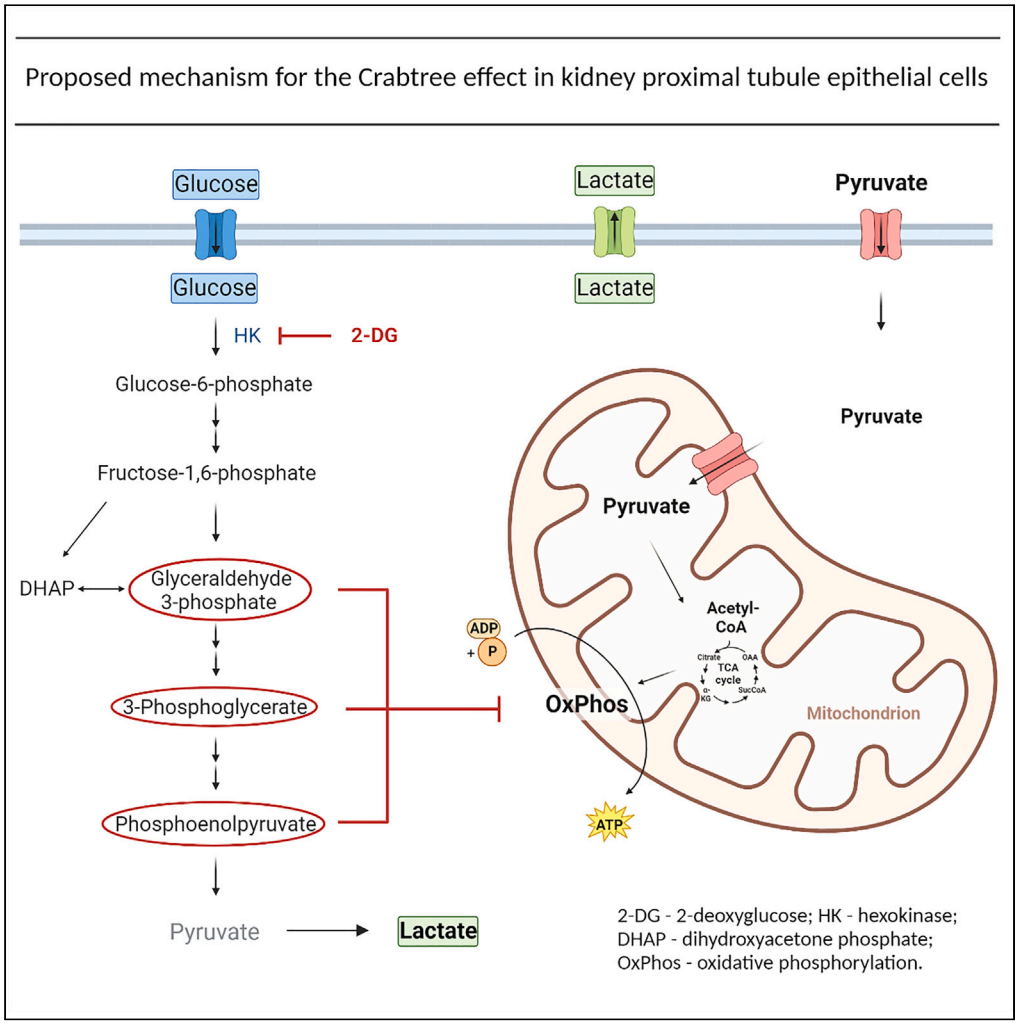

Manjula Darshi, Jana Tumova, Afaf Saliba, Jiwan Kim, Judy Baek, Subramaniam Pennathur, Kumar Sharma

sharmak3@uthscsa.edu

Highlights

Glucose triggers respiratory inhibition in PTEC

2-deoxyglucose reverses the Crabtree effect in PTEC

The Crabtree effect in PTEC is mediated by late-stage glycolytic intermediates

Darshi et al., iScience 26, 106462
April 21, 2023 © 2023
https://doi.org/10.1016/j.isci.2023.106462

iScience

CellPress
OPEN ACCESS

Article

Crabtree effect in kidney proximal tubule cells via late-stage glycolytic intermediates

Manjula Darshi,[1,5] Jana Tumova,[1,2,5] Afaf Saliba,[1] Jiwan Kim,[1,3] Judy Baek,[4] Subramaniam Pennathur,[4] and Kumar Sharma[1,6,*]

SUMMARY

The Crabtree effect is defined as a rapid glucose-induced repression of mitochondrial oxidative metabolism and has been described in yeasts and tumor cells. Using plate-based respirometry, we identified the Crabtree effect in normal (non-tumor) kidney proximal tubule epithelial cells (PTEC) but not in other kidney cells (podocytes or mesangial cells) or mammalian cells (C2C12 myoblasts). Glucose-induced repression of respiration was prevented by reducing glycolysis at the proximal step with 2-deoxyglucose and partially reversed by pyruvate. The late-stage glycolytic intermediates glyceraldehyde 3-phosphate, 3-phosphoglycerate, and phosphoenolpyruvate, but not the early-stage glycolytic intermediates or lactate, inhibited respiration in permeabilized PTEC and kidney cortex mitochondria, mimicking the Crabtree effect. Studies in diabetic mice indicated a pattern of increased late-stage glycolytic intermediates consistent with a similar pattern occurring *in vivo*. Our results show the unique presence of the Crabtree effect in kidney PTEC and identify the major mediators of this effect.

INTRODUCTION

While several recent studies have shown the pivotal role of chronic hyperglycemia and mitochondrial dysfunction in the pathogenesis of kidney disease,[1,2] time-dependent effects of glucose exposure per se on mitochondrial function of different kidney cells have not been well characterized. Reabsorption of glucose in kidneys takes place in proximal tubules and requires tremendous energy expenditure. Proximal tubule epithelial cells (PTEC) are constantly exposed to varying loads of glucose which require reabsorption, although the filtered glucose level is tightly controlled by insulin and systemic metabolism. Metabolic adaptations associated with marked fluctuations in glucose exposure likely play an important role in the normal function of these cells and in the development of pathological conditions during a disease state. Therefore, we focused on characterization of the effects related to different concentrations of glucose on cellular energy metabolism in PTEC.

The Crabtree effect is defined as the glucose-induced repression of mitochondrial oxidative metabolism and has originally been described in tumor cells[3] and broadly studied in yeasts. Crabtree is sometimes interchanged with the Warburg effect, which is a sustained preference of glycolysis in the presence of oxygen (so-called oxidative glycolysis) and is basically an inability of the cell to suppress glycolysis by oxidative metabolism despite the availability of oxygen.[4] The Warburg effect was first described in tumors[5] but has also been described in non-tumor cells and implicated in diabetic complications.[6] The Crabtree effect, in contrast to the Warburg effect, describes a rapid glucose-induced inhibition of oxygen consumption, in terms of seconds to minutes. The cells shift from energy-efficient aerobic respiration to less efficient glycolysis resulting in fermentation, culminating in ethanol production in yeast, and lactate production in mammalian cells. Despite decades of research, the mechanisms underlying the Crabtree effect are not clearly understood. The mechanisms proposed to underlie the Crabtree effect include decreased cytosolic phosphate concentration,[7] competition of glycolytic enzymes and mitochondria for free cytosolic ADP,[8] or accumulation of the glycolytic intermediate fructose-1,6-bisphosphate;[9,10] however, no unifying mechanism has been proven to date in normal mammalian cells. A major question as to why cells shift from energy-efficient oxidative phosphorylation to energy-inefficient glycolysis in the presence of glucose is also yet to be answered. Several explanations of this phenomenon were suggested for yeasts (reviewed in the study by de Alteriis et al.[11]). In tumor cells, the glycolytic switch could better support rapid

[1]Division of Nephrology, Department of Medicine, Center for Precision Medicine, University of Texas Health Science Center at San Antonio, San Antonio, TX 78229, USA

[2]Department of Pathophysiology, Faculty of Medicine in Pilsen, Charles University, 323 00 Pilsen, Czech Republic

[3]Cancer Program, Broad Institute of Harvard and MIT, Cambridge, MA 02142, USA

[4]Department of Internal Medicine-Nephrology and Molecular and Integrative Physiology, University of Michigan, Ann Arbor, MI 48109, USA

[5]These authors contributed equally

[6]Lead contact

*Correspondence: sharmak3@uthscsa.edu

https://doi.org/10.1016/j.isci.2023.106462

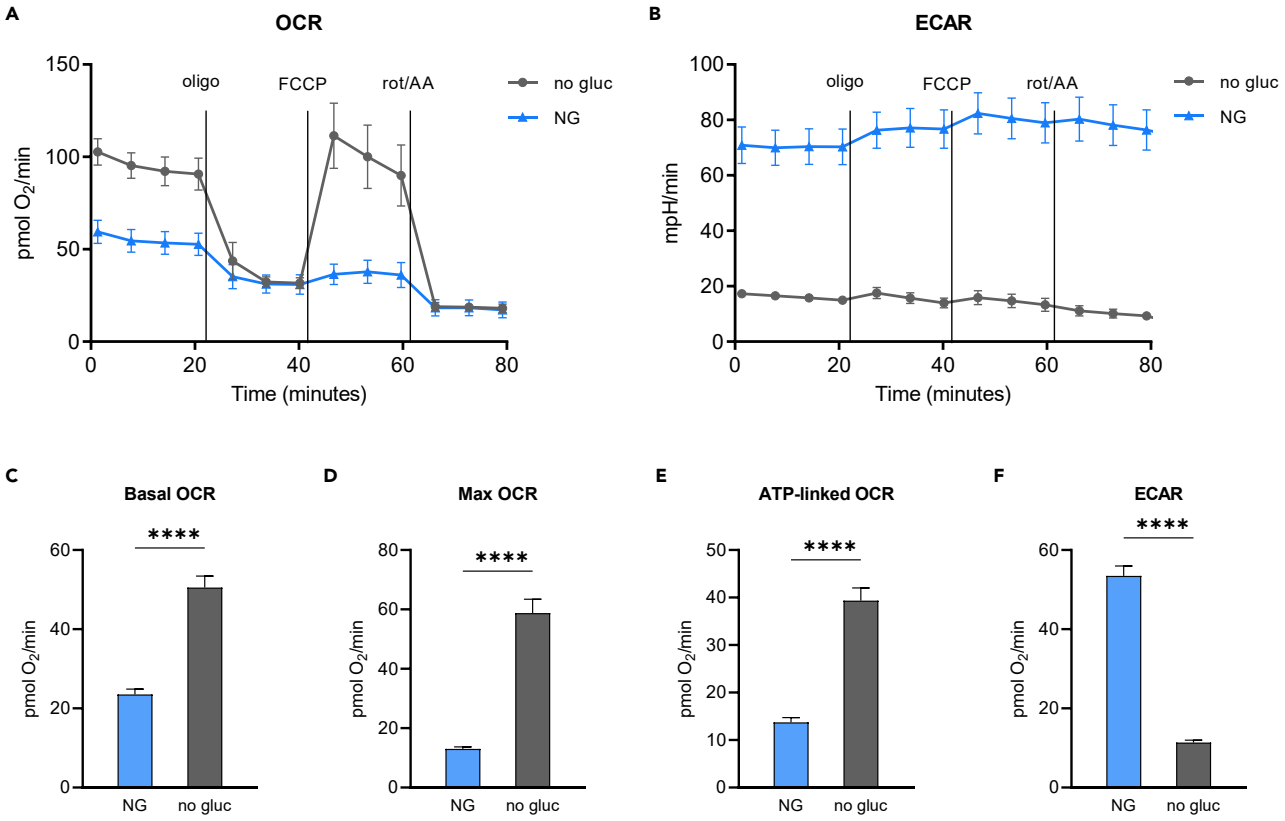

Figure 1. Glucose withdrawal significantly boost mitochondrial function in kidney PTEC

(A–F) HK-2 cells were grown in regular growth media (containing 5.8 mM glucose) and switched to assay media (Seahorse XF base medium with 5 mM HEPES) supplemented with no glucose (no gluc) or 5.5 mM glucose (NG) 1 h prior the assay. Changes in OCR and ECAR were measured before and after sequential injections of oligomycin, FCCP, and rotenone/antimycin A. (A and B) OCR and ECAR from a representative stress test experiment showing times of mitochondrial inhibitors addition. Data are represented as mean ± SD. (C–F) Basal OCR, maximal OCR, ATP-linked OCR, and ECAR calculated as described in STAR Methods section. Data are represented as mean ± SEM.****$p < 0.0001$ by Student's *t* test.

proliferation and need for macromolecular synthesis.[12] The same explanation applies for proliferating thymocytes, another cell type with reported Crabtree effect.[13]

In the current study, we sought to identify changes of cellular energy metabolism associated with exposure to different concentrations of glucose or glucose withdrawal in PTEC and other kidney and non-kidney mammalian cells. Interestingly, we found that the kidney proximal tubular cell had a robust Crabtree effect which was mediated via late-stage glycolytic intermediates.

RESULTS

Glucose withdrawal significantly boosts mitochondrial function in kidney PTEC

To determine the consequence of glucose withdrawal on mitochondrial function, HK-2 cells, a human cell line derived from normal proximal tubular epithelial cells, were grown in normal growth media, which contains 5.8 mM glucose, i.e. a normal level of glucose, and then switched to assay media containing no glucose or normal glucose (5.5 mM, NG) 1 h before the extracellular flux analysis. In the absence of glucose or other added supplements, the source of reducing equivalents for oxidative phosphorylation is the metabolism of endogenous substrates, and/or amino acids which are present in the assay media together with vitamins (details in STAR Methods). Cells switched to no glucose had significantly higher basal and maximal oxygen consumption rate (OCR), and ATP-linked OCR, compared to cells kept in NG (Figures 1A and 1C–1E). Glucose withdrawal significantly boosted mitochondrial function as there was more than a 2-fold increase in basal OCR and more than a 4-fold increase in maximal OCR. The rise in OCR was accompanied by an expected decrease in extracellular acidification rate (ECAR) after switching to no glucose media (Figures 1B and 1F).

Glucose exposure triggers profound respiratory inhibition in kidney PTEC but not in other kidney or mammalian non-tumor cells

As we observed an increase in OCR in HK-2 cells assayed in the absence of glucose, we sought to explore the effect of glucose on mitochondrial respiration more closely in these cells. As shown in Figures 2A–2E, when cells were switched to different glucose concentrations 1 h before the assay, respiratory inhibition was noticed in as low as 1 mM glucose compared to no glucose. Maximum inhibition was observed with 5.5 mM glucose, and there was no additional effect on OCR inhibition when increasing the glucose concentration above 5.5 mM. Glucose-induced decrease in basal respiration can be explained by decreased ATP-linked respiration rather than a proton leak (Figures 2C and 2D). A profound decrease in maximal OCR (uncoupled respiration) in cells exposed to glucose indicates an inhibition of electron transport chain (ETC). The drop in OCR was accompanied by a dose-dependent increase in ECAR. When galactose was used instead of glucose, no reduction of the OCR was observed compared to no glucose (Figure S1A). We next assessed if the respiratory inhibition is specific to glucose or whether other hexoses can induce the same effect. Following basal respiratory measurements, 5.5 mM of glucose, mannitol, sucrose, ribose, fructose, and maltose were injected through injection port A of XF cartridge, and respiratory rates were measured. As shown in Figures S1B–S1E, glucose injection acutely inhibited respiration and induced glycolysis within 6 min. None of the other sugars tested had a similar effect, supporting the notion that respiratory inhibition is specific to glucose. We also ruled out an osmotic effect as equimolar levels of mannitol did not suppress OCR.

Because HK-2 cells are transformed, we sought to determine if the Crabtree effect is common to PTEC or if it is a characteristic only of HK-2 cells. We tested glucose-induced respiratory changes in human primary renal proximal tubule epithelial cells (RPTEC) and freshly isolated mouse kidney proximal tubule cells. In RPTEC, there was significant suppression of basal and maximal respiration in response to 7.2 mM glucose, with further reduction observed with a higher concentration of glucose, and an expected increase in ECAR (Figures 2F–2H). Treatment of mouse primary proximal tubule cells with 5.5 mM glucose also resulted in an increase in ECAR and a reduction of basal OCR (Figures 2I and 2J) compared to no glucose treatment. Increasing concentration of glucose to 25 mM did not have any additional effect on respiratory inhibition compared to 5.5 mM glucose. Those results confirm that the Crabtree effect is a common characteristic of PTEC across species.

To address if other kidney cells exhibit the Crabtree effect similar to proximal tubule cells, we assayed OCR and ECAR in podocytes and mesangial cells under NG, high glucose (HG), and no glucose conditions. No significant changes were noted in basal respiration in podocytes. However, maximal respiration and ECAR were enhanced with both 5.5 and 25 mM glucose (Figures S2A and S2B). In mesangial cells, basal respiration was suppressed by glucose although to a lesser extent than in PTEC. However, maximal OCR was higher in both 5.5 and 25 mM glucose compared to no glucose indicating there was no inhibition of ETC by glucose (Figures S2C and S2D). To address if other mammalian non-tumor cell lines exhibit the Crabtree effect, we assayed C2C12 myoblasts under NG and no glucose conditions (Figures S2E and S2F). There was no inhibition of respiration observed and the addition of glucose significantly increased OCR compared to no glucose. Our data show that while glycolysis is expectedly upregulated in all tested cell types after glucose exposure, the increase in glycolysis is associated with respiratory inhibition uniquely in PTEC.

To determine if the Crabtree effect leads to ATP depletion in PTEC, we calculated rates of ATP production in the presence or absence of glucose.[14] Total ATP production rate was not decreased but even increased in NG compared to no glucose conditions (Figure 2L). Without glucose, 80% of the ATP was from oxidative phosphorylation, which was completely inverted in the presence of glucose, wherein 80% of the ATP was from glycolysis (Figure 2K). These data indicate that despite the profound reduction in respiration, cells in 5.5 mM glucose can generate the same or even higher amount of ATP through glycolysis as they did in no glucose conditions, even though glycolysis is much less efficient than oxidative phosphorylation. These results suggest that glucose induces an adaptive metabolic switch to glycolysis while suppressing oxidative phosphorylation specifically in PTEC.

Pyruvate partially and 2-deoxyglucose almost completely reverses the Crabtree effect in PTEC

HK-2 cells are typically cultured in K-SFM media which contains 5.8 mM glucose along with 0.6 mM pyruvate (Thermo Fisher Scientific). We tested if supplementing assay media with different pyruvate concentrations

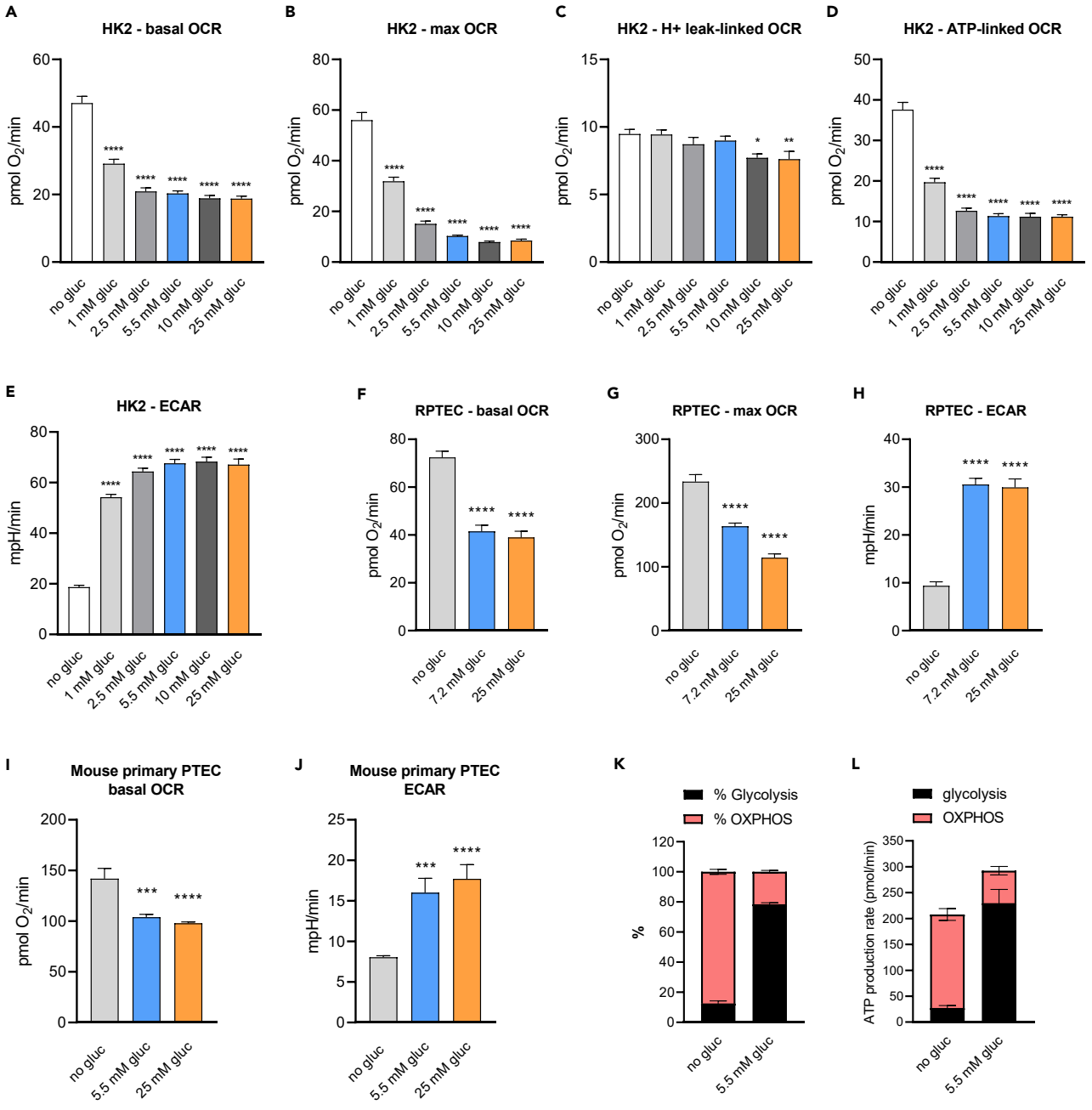

Figure 2. Glucose exposure triggers switch to glycolysis and profound respiratory inhibition in various kidney proximal tubule epithelial cells

(A–J) Basal OCR, maximal OCR, H+ leak, ATP-linked OCR, and ECAR in HK-2 cells (A–E), RPTEC (F–H), and mouse primary tubular cells (I and J) exposed to different concentrations of glucose. Cells were switched to assay media (Seahorse XF base medium with 5 mM HEPES) containing indicated concentration of glucose 1 h prior the assay. The assay media was supplemented with 1 mM pyruvate and 2 mM glutamine for mouse primary PTEC as they did not tolerate the absence of exogenous substrates. Changes in OCR and ECAR were measured before and after sequential injections of oligomycin, FCCP and rotenone/antimycin A.

(K and L) Seahorse XF Real-Time ATP Rate Assay to calculate rates of ATP production from oxidative phosphorylation (OXPHOS) and glycolysis in HK-2 cells in NG compared to no glucose assay media. Data are represented as mean ± SEM. *$p < 0.05$, **$p < 0.01$, ***$p < 0.001$, ****$p < 0.0001$ compared to no glucose by one-way ANOVA followed by Dunnett's post-hoc test for multiple comparisons. See also Figures S1 and S2.

can circumvent the Crabtree effect. Respiratory rates were measured in XF assay media with or without 5.5 mM glucose along with pyruvate in the concentration range of 0.5–3 mM (Figures 3A–3C). Adding increasing concentrations of pyruvate to NG media had a minor effect on basal respiratory rates when compared to NG only. However, pyruvate addition significantly improved maximal respiratory rates in a dose-dependent manner, starting at 0.5 mM concentration and reaching a maximum effect at 2 mM concentration. This demonstrates that pyruvate addition does not affect the basal respiration linked to ATP production but can improve the maximal capacity of the electron transport chain, which is suppressed by glucose. However, 2 mM pyruvate concentration can be considered supraphysiological and is not commonly used in cell culture.

2-deoxyglucose (2-DG) is a competitive inhibitor of hexokinase that reduces the initial conversion of glucose to glucose 6-phosphate and the overall rate of glycolysis. The addition of 2-DG to HK-2 cells in 5.5 mM glucose reduced the ECAR in a dose-dependent manner and restored the glucose-induced reduction of both basal and maximal OCR, with an effective dose starting at 5.5 mM and maximal effect achieved with 25 mM concentration (Figures 3D and 3H). The fact that inhibition of the early-stage of glycolysis with 2-DG ameliorated the drop of respiration caused by glucose indicates that glycolysis itself is inducing the Crabtree effect.

The Crabtree effect in PTEC is mediated by late-stage glycolytic intermediates

To determine the levels of glycolytic intermediates in different glucose conditions, HK-2 cells were switched from growth media to assay media containing no glucose, NG, or HG for 1 h and mass spec analysis of glycolytic intermediates was performed in cell extracts. Early and late-stage glycolytic intermediates, and lactate were increased in NG and HG compared to no glucose conditions, while there was a decrease in pyruvate levels (Figure S3). To determine if glycolytic intermediates are involved in the inhibition of mitochondrial respiration, permeabilized HK-2 cells were treated with 5 mM glucose or each of the glycolytic intermediates. Glucose itself and lactate, the end-product of glycolysis, had no effect on state 3 respiratory rates (phosphorylating respiration) in permeabilized cells. Glucose-6-phosphate (G6P) and fructose 1,6-bisphosphate (F1,6BP), the early-stage glycolytic intermediates also had no effect on state 3 respiratory rates (Figure 4A). Surprisingly, the late-stage glycolytic intermediates, glyceraldehyde 3-phosphate (G3P), 3-phosphoglycerate (3 PG), and phosphoenolpyruvate (PEP) all significantly decreased respiration in permeabilized cells (Figure 4A).

Glycolytic intermediates are increased in diabetic mouse kidneys and late-stage glycolytic intermediates suppress respiration in kidney cortex mitochondria

To determine if the pattern of increased glycolytic intermediates is also seen in an *in vivo* situation where the load of glucose in PTEC is increased, we performed mass spec analysis of glycolytic intermediates in kidney cortex of db/db mice. The db/db mouse is a well-established animal model of type 2 diabetes. We found an increase in all glycolytic intermediates, except for G6P, in the kidney cortex of diabetic mice compared to wild-type (WT) mice (Figure 4C). The levels of G3P were below the detection limit so the levels of DHAP are shown. To determine the effect of glycolytic intermediates on respiration in tissue mitochondria, kidney cortex mitochondria were isolated from WT mice and treated with 5 mM glucose or each of the glycolytic intermediates. Similar to permeabilized cells, glucose, lactate, and early-stage glycolytic intermediates had no effect on state 3 respiration, while the late-stage glycolytic intermediates G3P, 3 PG, and PEP all significantly decreased state 3 respiration (Figure 4B).

DISCUSSION

We show, to our knowledge, for the first time that normal (non-tumor) kidney PTEC exhibit the Crabtree effect even at low physiological concentrations of glucose. The glucose-induced respiratory inhibition is reversible and can be recovered by withdrawing glucose or inhibition of glycolysis. The mediators of the Crabtree effect in kidney PTEC are the late-stage glycolytic intermediates, while early-stage glycolytic intermediates or lactate do not have any significant effect on mitochondrial respiration. Our studies in different cell types further indicate that the Crabtree effect appears to be unique to PTEC as it was not observed in other kidney cell types, or in muscle cells.

Considering the fast switch (in order of minutes) from glycolysis to respiration and vice versa based on glucose availability in PTEC, we can exclude the role of changes in mitochondrial protein content related

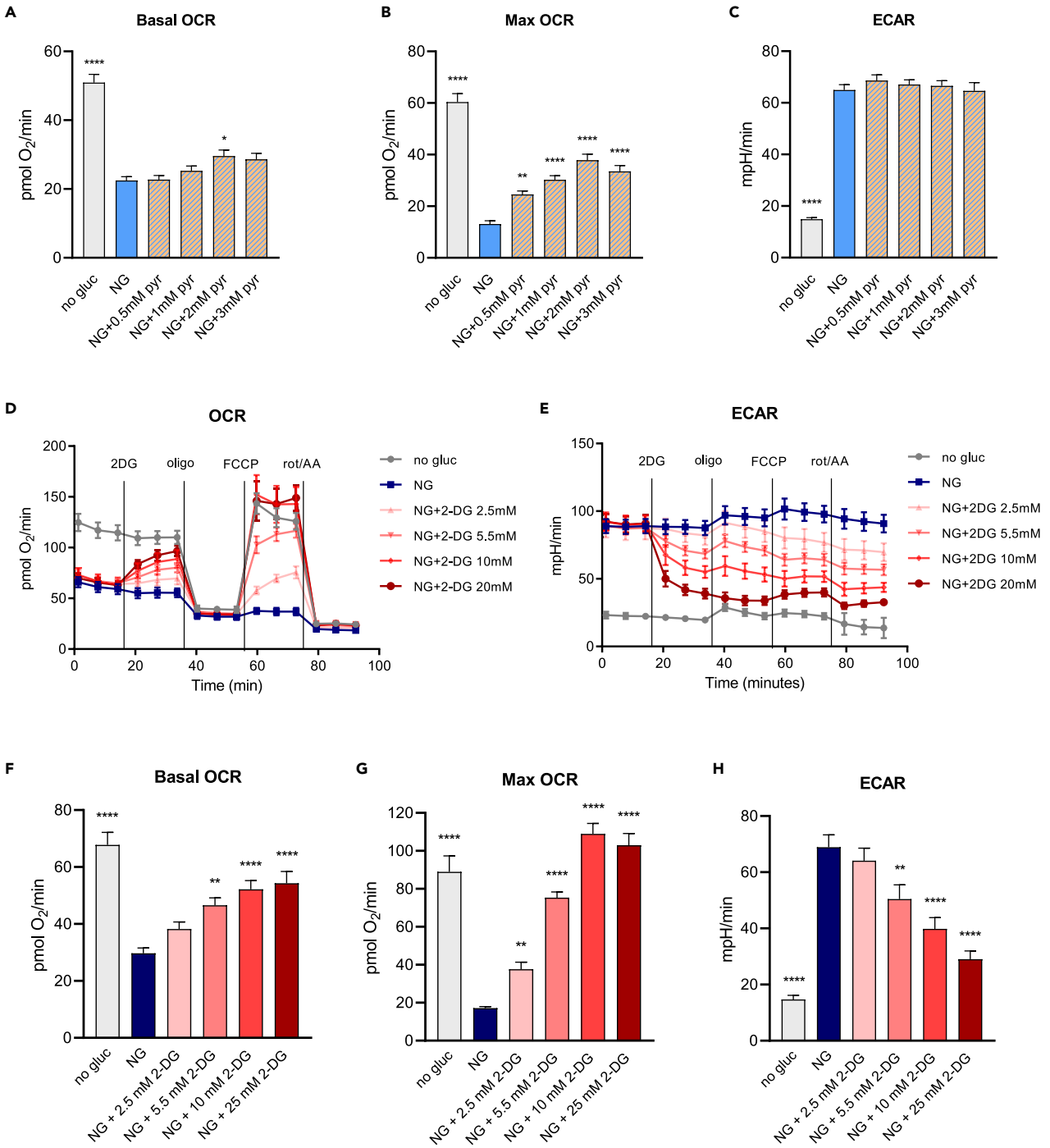

Figure 3. Pyruvate partially and 2-DG almost completely reverses the Crabtree effect in PTEC

(A–C) HK-2 cells were switched to assay media (Seahorse XF base medium with 5 mM HEPES) with indicated concentration of glucose along with pyruvate in concentration range of 0.5–3 mM 1 h prior the assay. Changes in OCR and ECAR were measured before and after sequential injections of oligomycin, FCCP, and rotenone/antimycin A. Data are represented as mean ± SEM.

(D and E) HK-2 cells were switched to assay media with no glucose or 5.5 mM glucose 1 h prior the assay and indicated concentrations of 2-DG were injected to cells following rate 3 through XF cartridge port A followed by injections of oligomycin, FCCP, and rotenone + antimycin A. Data are shown as mean ± SD from a representative experiment.

(F–H) Basal OCR, maximal OCR, and ECAR calculated as described in STAR Methods section. Data are represented as mean ± SEM. *$p < 0.05$, **$p < 0.01$, ***$p < 0.001$, ****$p < 0.0001$ compared to NG by one-way ANOVA followed by Dunnett's post-hoc test for multiple comparisons.

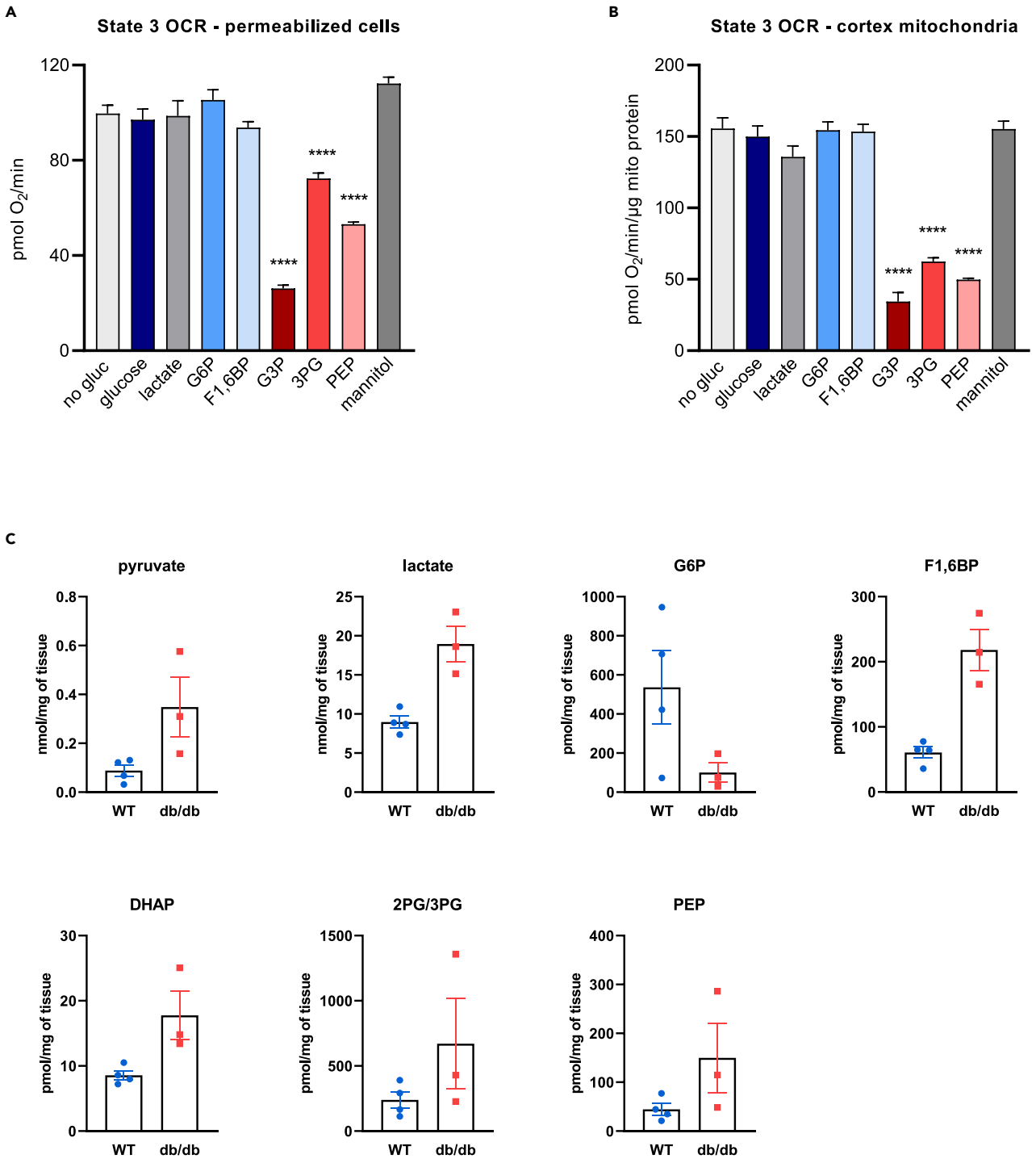

Figure 4. Late-stage glycolytic intermediates mimic the Crabtree effect in permeabilized PTEC and kidney cortex mitochondria; glycolytic intermediates are increased in diabetic mouse kidneys

(A and B) State 3 respiratory rates (phosphorylating respiration) in permeabilized HK-2 cells and kidney cortex mitochondria assayed in MAS buffer supplemented with 0.5 mM pyruvate and 0.5 mM malate as substrates, 4 mM ADP and 5 mM concentration of indicated compounds. Data are represented as mean ± SEM. ****$p < 0.0001$ compared to no glucose by one-way ANOVA followed by Dunnett's post-hoc test for multiple comparisons.

(C) 6-months-old C57BL/6J mice (WT, n = 4) and 5-months-old type 2 diabetic mice (db/db, n = 3) were sacrificed, their kidneys harvested and kidney cortex processed for mass spec analysis of glycolytic intermediates. Data are represented as mean ± SEM. See also Figure S3.

to changes in gene expression. The decrease in uncoupled respiratory rate after glucose treatment indicates an inhibition of mitochondrial respiratory chain as a mediator/trigger of the Crabtree effect rather than the decreased cytosolic ADP and phosphate (Pi) levels as previously suggested.[7,8] The restoration of maximal respiratory capacity after removing glucose from the media points to a short-term reversible functional adaptation mechanism, which appears to be distinguished from the Warburg effect due to long-term metabolic reprogramming.[15] Another previously reported mechanism mediating the Crabtree effect is the direct regulation of mitochondrial respiratory chain by early-stage glycolytic intermediate F1,6BP.[9,10] Inhibition of respiration by this early-stage glycolytic intermediate was shown in yeasts and uniquely also in isolated rat liver mitochondria.[9] Contrary to those studies, we did not observe any inhibitory effect of the early-stage glycolytic intermediates (G6P and F1,6BP) on mitochondrial respiration using permeabilized PTEC and isolated mouse kidney cortex mitochondria. However, we did see a profound effect of late-stage glycolytic intermediates, G3P, 3 PG, and PEP suggesting that late-stage intermediates do play a key mechanistic role in the Crabtree effect in PTEC.

High rates of glycolysis are associated with increased lactate production, as described in highly proliferating cells,[12,16] leading to a decreased mitochondrial pyruvate oxidation. It could be assumed that pyruvate supplementation might rescue the respiration inhibited by glucose-induced glycolytic flux. However, even at supraphysiological concentrations, pyruvate did not prevent the inhibition of basal respiration by glucose and only partially prevented the inhibition of maximal respiration in PTEC. In contrast, 2-DG completely reversed the Crabtree effect in PTEC suggesting a potential involvement of glycolytic metabolites in respiratory inhibition. The potent effect of 2-DG may contribute to the protective effect of 2-DG in models of kidney disease progression or acute kidney injury.[17,18] Interestingly, the diabetic condition is associated with an increase in pyruvate, lactate, and early and late-stage glycolytic intermediates. Of these, only the late-stage glycolytic intermediates inhibit respiration in mouse proximal tubular cells and in intact mitochondria from normal mouse kidneys. The mechanism as to how late-stage glycolytic intermediates suppress mitochondrial respiration is the focus of our future studies.

Another question is why PTEC shift from energy-efficient respiration to energy-inefficient glycolysis in the presence of glucose. In distinction to cancer cells that switch to anaerobic glycolysis due to their fast proliferation and need for macromolecular synthesis,[12] one would not expect proliferation to be a driving force in PTEC exposed to glucose. One possible explanation may be that the Crabtree effect is an adaptive mechanism of proximal tubular cells to protect mitochondria against increased reactive oxygen species (ROS) production and oxidative damage. Limiting oxidative phosphorylation in proximal tubular cells may prevent ROS production and ROS-mediated mtDNA damage, as described in yeast.[19] However, our data do not support this hypothesis as normal glucose condition compared to no glucose condition was not associated with decreased proton leak, i.e. uncoupled respiration leading to ROS production, but rather decreased respiration linked to ATP turnover in PTEC. More data would be needed to clarify the potential role of Crabtree in decreasing ROS production and cellular damage.

Inefficient ATP production via oxidative glycolysis may be a problem when resources are scarce, which is not the case for cultured cells.[12] In agreement with this statement, we have shown that ATP production rate is not decreased with glucose compared to the no glucose conditions. Glycolysis is able to supply sufficient ATP to cover cellular needs and the Crabtree effect may be may be triggered to preserve cellular homeostasis in conditions where glucose uptake is higher than processing capability of the second phase of glycolysis.[11] However, *in vivo*, if a similar process occurs, cells will reach a state of complete dependency on glycolytic metabolism, and oxidative phosphorylation will be under-utilized. Robust glycolysis may be sufficient to avoid organ injury but leaves the cells susceptible to a variety of environmental stressors that challenge the cell's ability to maintain its energetic needs. Therefore, pathways that promote restoration of oxidative phosphorylation may bring back bioenergetic versatility to proximal tubular cells.

We confirmed our observation on several PTEC, including RPTEC and freshly isolated mouse PTEC. The kidney cortex of diabetic mice shows a similar pattern of increased late-stage glycolytic intermediates suggesting their role in kidney damage associated with high glucose load as seen in diabetes. Our observation is supported by previous work[1] where targeted metabolomic analysis on kidney cortex showed that the levels of late-stage but not early-stage glycolytic intermediates are increased in the 24-weeks-old db/db mice compared to the WT mice. The role of pseudohypoxia in the diabetic condition could contribute to the Crabtree effect in kidney proximal tubular cells.[20]

In summary, we show an important, not yet described, metabolic feature of kidney PTEC and identify the mediators of this effect, the late-stage glycolytic intermediates. We propose that a similar effect may be seen in *in vivo* situation in diabetic kidneys, and that increased levels of late-stage glycolytic intermediates may be responsible for suppression of mitochondrial function and kidney damage. Further studies will be necessary to find mechanism as to how late-stage glycolytic intermediates suppress mitochondrial respiration and may contribute to progressive kidney disease *in vivo*.

Limitations of study

We were able to identify the Crabtree effect presence in PTEC and the mediators of this effect. However, why PTEC shift from energy-efficient respiration to energy-inefficient glycolysis in the presence of glucose is not clear from our experiments. We speculate that it is a metabolic adaptation associated with marked fluctuations in glucose exposure which happens in PTEC. With persistent exposure to excess glucose, the Crabtree effect could be deleterious to the proximal tubular cell and neighboring cells. Another limitation is that we have not addressed the involvement of glucose transporters and metabolites transporters in the Crabtree effect and this will be the focus of our future studies. Similarly, it would be interesting to see if the effect is specific for proximal vs distal tubules, a question we will try to answer with single cell omics studies.

STAR★METHODS

Detailed methods are provided in the online version of this paper and include the following:

- KEY RESOURCES TABLE
- RESOURCE AVAILABILITY
  - Lead contact
  - Materials availability
  - Data and code availability
- EXPERIMENTAL MODEL AND SUBJECT DETAILS
  - Animals
  - Cell culture
- METHOD DETAILS
  - Isolation of mouse kidney cortex mitochondria
  - Respiration and glycolysis measurements
  - Glycolytic intermediates quantification by mass spectrometry
- QUANTIFICATION AND STATISTICAL ANALYSIS

SUPPLEMENTAL INFORMATION

Supplemental information can be found online at https://doi.org/10.1016/j.isci.2023.106462.

ACKNOWLEDGMENTS

A.S. was supported by NIH/NCATS, TL1 TR002647. J.B. and S.P. were supported by 5F30DK121463, R24DK082841, P30 DK081943, P30 DK89503 and JDRF Center for Excellence 5-COE-2019-861-S-B. J.T. and M.D. were supported in part by VA Merit grants to K.S. and R24DK082841 (S.P. and K.S.). The graphical abstract was created with Biorender.com.

AUTHOR CONTRIBUTIONS

Conceptualization, J.T., M.D., and K.S.; Methodology, J.T. and M.D.; Validation, J.T.; Formal Analysis, J.T. and M.D.; Investigation, J.T., M.D., A.S., J.K., and J.B.; Writing-Original Draft, J.T. and M.D.; Writing-Review & Editing, J.T., M.D., J.K., A.S., J.B., S.P., and K.S.; Visualization, J.T., M.D., A.S., and J.K.; Supervision, S.P. and K.S.; Funding Acquisition, S.P. and K.S.

DECLARATION OF INTERESTS

The authors declare no competing interests.

INCLUSION AND DIVERSITY

We support inclusive, diverse, and equitable conduct of research.

Received: January 13, 2023
Revised: February 17, 2023
Accepted: March 17, 2023
Published: March 21, 2023

REFERENCES

1. Sas, K.M., Kayampilly, P., Byun, J., Nair, V., Hinder, L.M., Hur, J., Zhang, H., Lin, C., Qi, N.R., Michailidis, G., et al. (2016). Tissue-specific metabolic reprogramming drives nutrient flux in diabetic complications. JCI Insight *1*, e86976. https://doi.org/10.1172/jci.insight.86976.

2. Sharma, K., Karl, B., Mathew, A.V., Gangoiti, J.A., Wassel, C.L., Saito, R., Pu, M., Sharma, S., You, Y.H., Wang, L., et al. (2013). Metabolomics reveals signature of mitochondrial dysfunction in diabetic kidney disease. J. Am. Soc. Nephrol. *24*, 1901–1912. https://doi.org/10.1681/ASN.2013020126.

3. Crabtree, H.G. (1929). Observations on the carbohydrate metabolism of tumours. Biochem. J. *23*, 536–545. https://doi.org/10.1042/bj0230536.

4. Barros, L.F., Ruminot, I., San Martín, A., Lerchundi, R., Fernández-Moncada, I., and Baeza-Lehnert, F. (2021). Aerobic glycolysis in the brain: Warburg and crabtree contra pasteur. Neurochem. Res. *46*, 15–22. https://doi.org/10.1007/s11064-020-02964-w.

5. Warburg, O. (1925). The metabolism of carcinoma Cells1. J. Cancer Res. *9*, 148–163. https://doi.org/10.1158/jcr.1925.148.

6. Zhang, G., Darshi, M., and Sharma, K. (2018). The Warburg effect in diabetic kidney disease. Semin. Nephrol. *38*, 111–120. https://doi.org/10.1016/j.semnephrol.2018.01.002.

7. Koobs, D.H. (1972). Phosphate mediation of the crabtree and pasteur effects. Science *178*, 127–133. https://doi.org/10.1126/science.178.4057.127.

8. Rodríguez-Enríquez, S., Juárez, O., Rodríguez-Zavala, J.S., and Moreno-Sánchez, R. (2001). Multisite control of the Crabtree effect in ascites hepatoma cells. Eur. J. Biochem. *268*, 2512–2519. https://doi.org/10.1046/j.1432-1327.2001.02140.x.

9. Díaz-Ruiz, R., Avéret, N., Araiza, D., Pinson, B., Uribe-Carvajal, S., Devin, A., and Rigoulet, M. (2008). Mitochondrial oxidative phosphorylation is regulated by fructose 1,6-bisphosphate. A possible role in Crabtree effect induction? J. Biol. Chem. *283*, 26948–26955. https://doi.org/10.1074/jbc.M800408200.

10. Rosas Lemus, M., Roussarie, E., Hammad, N., Mougeolle, A., Ransac, S., Issa, R., Mazat, J.P., Uribe-Carvajal, S., Rigoulet, M., and Devin, A. (2018). The role of glycolysis-derived hexose phosphates in the induction of the Crabtree effect. J. Biol. Chem. *293*, 12843–12854. https://doi.org/10.1074/jbc.RA118.003672.

11. de Alteriis, E., Cartenì, F., Parascandola, P., Serpa, J., and Mazzoleni, S. (2018). Revisiting the Crabtree/Warburg effect in a dynamic perspective: a fitness advantage against sugar-induced cell death. Cell Cycle *17*, 688–701. https://doi.org/10.1080/15384101.2018.1442622.

12. Vander Heiden, M.G., Cantley, L.C., and Thompson, C.B. (2009). Understanding the Warburg effect: the metabolic requirements of cell proliferation. Science *324*, 1029–1033. https://doi.org/10.1126/science.1160809.

13. Greiner, E.F., Guppy, M., and Brand, K. (1994). Glucose is essential for proliferation and the glycolytic enzyme induction that provokes a transition to glycolytic energy production. J. Biol. Chem. *269*, 31484–31490.

14. Mookerjee, S.A., Gerencser, A.A., Nicholls, D.G., and Brand, M.D. (2018). Quantifying intracellular rates of glycolytic and oxidative ATP production and consumption using extracellular flux measurements. J. Biol. Chem. *293*, 12649–12652. https://doi.org/10.1074/jbc.AAC118.004855.

15. Diaz-Ruiz, R., Rigoulet, M., and Devin, A. (2011). The Warburg and Crabtree effects: on the origin of cancer cell energy metabolism and of yeast glucose repression. Biochim. Biophys. Acta *1807*, 568–576. https://doi.org/10.1016/j.bbabio.2010.08.010.

16. DeBerardinis, R.J., Lum, J.J., Hatzivassiliou, G., and Thompson, C.B. (2008). The biology of cancer: metabolic reprogramming fuels cell growth and proliferation. Cell Metabol. *7*, 11–20. https://doi.org/10.1016/j.cmet.2007.10.002.

17. Rowe, I., Chiaravalli, M., Mannella, V., Ulisse, V., Quilici, G., Pema, M., Song, X.W., Xu, H., Mari, S., Qian, F., et al. (2013). Defective glucose metabolism in polycystic kidney disease identifies a new therapeutic strategy. Nat. Med. *19*, 488–493. https://doi.org/10.1038/nm.3092.

18. Tan, C., Gu, J., Li, T., Chen, H., Liu, K., Liu, M., Zhang, H., and Xiao, X. (2021). Inhibition of aerobic glycolysis alleviates sepsis-induced acute kidney injury by promoting lactate/Sirtuin 3/AMPK-regulated autophagy. Int. J. Mol. Med. *47*, 19. https://doi.org/10.3892/ijmm.2021.4852.

19. Chen, Z., Odstrcil, E.A., Tu, B.P., and McKnight, S.L. (2007). Restriction of DNA replication to the reductive phase of the metabolic cycle protects genome integrity. Science *316*, 1916–1919. https://doi.org/10.1126/science.1140958.

20. Song, J., Yang, X., and Yan, L.J. (2019). Role of pseudohypoxia in the pathogenesis of type 2 diabetes. Hypoxia *7*, 33–40. https://doi.org/10.2147/HP.S202775.

21. Ryan, M.J., Johnson, G., Kirk, J., Fuerstenberg, S.M., Zager, R.A., and Torok-Storb, B. (1994). HK-2: an immortalized proximal tubule epithelial cell line from normal adult human kidney. Kidney Int. *45*, 48–57. https://doi.org/10.1038/ki.1994.6.

22. Eid, A.A., Lee, D.Y., Roman, L.J., Khazim, K., and Gorin, Y. (2013). Sestrin 2 and AMPK connect hyperglycemia to Nox4-dependent endothelial nitric oxide synthase uncoupling and matrix protein expression. Mol. Cell Biol. *33*, 3439–3460. https://doi.org/10.1128/MCB.00217-13.

23. Das, F., Ghosh-Choudhury, N., Lee, D.Y., Gorin, Y., Kasinath, B.S., and Choudhury, G.G. (2018). Akt2 causes TGFbeta-induced deptor downregulation facilitating mTOR to drive podocyte hypertrophy and matrix protein expression. PLoS One *13*, e0207285. https://doi.org/10.1371/journal.pone.0207285.

24. Ding, W., Yousefi, K., and Shehadeh, L.A. (2018). Isolation, characterization, and high throughput extracellular flux analysis of mouse primary renal tubular epithelial cells. J. Vis. Exp. *136*, 57718. https://doi.org/10.3791/57718.

25. Rogers, G.W., Brand, M.D., Petrosyan, S., Ashok, D., Elorza, A.A., Ferrick, D.A., and Murphy, A.N. (2011). High throughput microplate respiratory measurements using minimal quantities of isolated mitochondria. PLoS One *6*, e21746. https://doi.org/10.1371/journal.pone.0021746.

26. Brand, M.D., and Nicholls, D.G. (2011). Assessing mitochondrial dysfunction in cells. Biochem. J. *435*, 297–312. https://doi.org/10.1042/BJ20110162.

27. Nakayasu, E.S., Nicora, C.D., Sims, A.C., Burnum-Johnson, K.E., Kim, Y.M., Kyle, J.E., Matzke, M.M., Shukla, A.K., Chu, R.K., Schepmoes, A.A., et al. (2016). MPLEx: a robust and universal protocol for single-sample integrative proteomic, metabolomic, and lipidomic analyses. mSystems *1*, e00043–e00116. https://doi.org/10.1128/mSystems.00043-16.

28. Baek, J., and Pennathur, S. (2021). Urinary 2-hydroxyglutarate enantiomers are markedly elevated in a murine model of type 2 diabetic kidney disease. Metabolites *11*, 469. https://doi.org/10.3390/metabo11080469.

STAR★METHODS

KEY RESOURCES TABLE

REAGENT or RESOURCE	SOURCE	IDENTIFIER
Chemicals, peptides, and recombinant proteins		
Keratinocyte serum-free media (K-SFM)	Thermo Fisher Scientific	17005042
Renal Epithelial Cell Growth Medium (REGM)	Lonza	CC-3190
Penicillin-Streptomycin	Thermo Fisher Scientific	15140122
Collagenase IV	Sigma-Aldrich	C5138
Collagen Coating Solution	Sigma-Aldrich	125-50
XF base medium without phenol red	Agilent	103335-100
Oligomycin	Sigma-Aldrich	75351
Carbonyl cyanide 4-(trifluoromethoxy) phenylhydrazone (FCCP)	Sigma-Aldrich	C2920
Rotenone	Sigma-Aldrich	R8875
Antimycin A	Sigma-Aldrich	A8674
Seahorse XF Plasma Membrane Permeabilizer	Agilent	02504-100
D-Glucose-6-Phosphate sodium salt (G6P)	Sigma-Aldrich	G7879
D-Fructose 1,6-bisphosphate trisodium salt hydrate (F1,6BP)	Sigma-Aldrich	F6803
D-Glyceraldehyde-3-phosphate solution (G3P)	Sigma-Aldrich	39705
D-(-)-3-Phosphoglyceric Acid (sodium salt) (3PG)	Cayman Chemical	20123
Phospho(enol)pyruvic acid monosodium salt hydrate (PEP)	Sigma-Aldrich	P0564
L-(+)-Lactic acid	Sigma-Aldrich	L1750
Glucose	Thermo Fisher Scientific	A24940-01
2-deoxy-D-glucose (2-DG)	Sigma-Aldrich	D8375
Critical commercial assays		
Seahorse XF FluxPak (cartridges, microplates, calibrant)	Agilent	02416-100
Seahorse XF Real-Time ATP Rate Assay Kit	Agilent	103592-100
Pierce™ BCA Protein Assay Kit	Thermo Fisher Scientific	23227
Experimental models: Cell lines		
Human kidney-2 (HK-2), Male	ATCC	CRL-2190, RRID:CVCL_0302
Human Renal Proximal Tubule Epithelial Cells (RPTEC), Female	Lonza	CC-2553-0000560580
Rat glomerular visceral epithelial cells (podocytes)	Laboratory of Dr. Yves Gorin	N/A (details published in Mol Cell Biol 2013 Vol. 33 Issue 17 Pages 3439-60- https://doi.org/10.1128/MCB.00217-13)
Rat mesangial cells	Laboratory of Dr. Yves Gorin	N/A (details published in PLoS One 2018 Vol. 13 Issue 11 Pages e0207285- https://doi.org/10.1371/journal.pone.0207285)
C2C12, Female	ATCC	CRL-1772, RRID:CVCL_0188
Experimental models: Organisms/strains		
C57BL/6J mice, males	The Jackson Laboratory	RRID:IMSR_JAX:000664
BKS.Cg-Dock7^{m} +/+ Lepr^{db}/J mice (db/db), males	The Jackson Laboratory	RRID:IMSR_JAX:000642
Software and algorithms		
Agilent Seahorse XF WAVE	Agilent	https://www.agilent.com
Seahorse XF Real-Time ATP Rate Assay Report Generator	Agilent	https://www.agilent.com
Mass Hunter Q-TOF Quantitative Analysis version B.07.01 Software	Agilent	https://www.agilent.com
Prism 9 GraphPad	GraphPad	https://www.graphpad.com

(*Continued on next page*)

Continued

REAGENT or RESOURCE	SOURCE	IDENTIFIER
Other		
Seahorse XFe96 Analyzer	Agilent	N/A
Agilent 6456 quadrupole time-of-flight (Q-TOF) mass spectrometer coupled to Agilent 1290 High-performance liquid chromatography	Agilent	N/A

RESOURCE AVAILABILITY

Lead contact

Further information and requests for resources and reagents should be directed to and will be fulfilled by the lead contact, Kumar Sharma (sharmak3@uthscsa.edu).

Materials availability

This study did not generate new unique reagents.

Data and code availability

- All data reported in this paper will be shared by the lead contact upon request.
- This paper does not report original code.
- Any additional information required to reanalyze the data reported in this paper is available from the lead contact upon request.

EXPERIMENTAL MODEL AND SUBJECT DETAILS

Animals

C57BL/6J (WT) mice (stock #000664, RRID:IMSR_JAX:000664) and BKS.Cg-Dock7m+/+ Leprdb/J (db/db) mice (stock #000642, RRID:IMSR_JAX:000642) were obtained from Jackson Laboratory. Mice were housed in the university's animal facility, which was maintained under normal humidity and temperature with 12 h periods of light and darkness. Food and water were provided *ad libitum*. All animal experiments were conducted with the approval of University of Texas Health Science Center at San Antonio (UTHSCSA) Institutional Animal Care and Use Committee (IACUC).

Cell culture

Human kidney proximal tubule epithelial cells (HK-2, ATCC® CRL-2190™, RRID:CVCL_0302)[21] were cultured and passaged as per ATCC recommendations. Cells were maintained in keratinocyte serum-free media (K-SFM) supplemented with 0.05 mg/ml bovine pituitary extract and 5 ng/ml epidermal growth factor (Thermo Fisher Scientific, 17005042) and sub-cultured at 80% confluency, typically once in 5 days. The concentration of glucose in K-SFM was 5.8 mM. The human renal proximal tubule epithelial cells (RPTEC; Lonza, CC-2553) were maintained in Renal Epithelial Cell Growth Medium (REGM) supplemented with 0.5% FBS, 5 μg/mL insulin, and 0.5 mL of hEGF, hydrocortisone, GA-1000, transferrin, T3, and epinephrine (Lonza, CC-3190). The concentration of glucose in REGM was 7.2 mM. Rat glomerular visceral epithelial cells (podocytes) and rat mesangial cells were generous gifts from the laboratory of the late Dr. Yves Gorin at UT Health Science Center at San Antonio and were cultured in Dulbecco's modified essential medium (DMEM) supplemented with 10% fetal bovine serum as previously described.[22,23] Mouse myoblasts (C2C12, ATCC® CRL-1772™, RRID:CVCL_0188) were cultured in high glucose DMEM supplemented with 10% fetal calf serum. All cell lines were cultured under 5% CO_2 at 37°C under a humidified atmosphere.

Primary renal tubular epithelial cells were isolated from 8-10 week old male C57BL/6J mice (The Jackson Laboratory, 000664, RRID:IMSR_JAX:000664) according to published protocols[24] (Ding et al., 2018) with minor modifications. Briefly, following cervical dislocation, both kidneys were extracted and placed on ice. Cortical regions were separated, chopped finely, washed with PBS containing 10% Penicillin-Streptomycin (Thermo Fisher Scientific) and treated with Collagenase IV (Sigma) for 30 minutes in 37 ^{0}C incubator with gentle shaking. The digested tissue was filtered through a 70 μm filter, resuspended in

REGM, and centrifuged at 50 g for 5 minutes at RT. The pellet was resuspended in 5 ml REGM and the supernatant was centrifuged at 50 g for 5 minutes at RT to ensure all tubular cells are collected into the second pellet. The second pellet was resuspended in 5 ml REGM. Both pellets' suspensions were combined in a tube containing 10 ml REGM (total of 20 ml) and centrifuged at 50 g for 5 minutes at RT. The final pellet was resuspended in 2 ml of REGM and plated on a T25 flask precoated with collagen coating solution (Sigma-Aldrich). Cells were cultured under 5% CO_2 at 37°C; media was changed every 48 h and after 8-10 days, tubular cells were passaged for further application. All experiments were done with passage 1 cells. T25 flasks were precoated with 2 ml collagen coating solution for 1 h at 37°C (placed in the cell culture incubator) and washed twice with sterile water and once with REGM media. The media was aspirated completely, and the flask was placed at the incubator until use.

METHOD DETAILS

Isolation of mouse kidney cortex mitochondria

Mitochondria were isolated from 8 -10 week old male C57BL/6J mice (The Jackson Laboratory, 000664, RRID:IMSR_JAX:000664) according to the published protocol.[25] Following a cervical dislocation, both kidneys were extracted and placed on ice and all subsequent steps of the preparation were performed on ice. Cortical regions were separated, chopped finely, and rinsed several times in MSHE (70 mM sucrose, 210 mM mannitol, 5 mM HEPES, 1 mM EGTA, and 0.5% (w/v) fatty acid-free BSA, pH 7.2) to remove blood. Tissue was disrupted using Teflon-glass Dounce homogenizer. The homogenate was centrifuged at 800 g for 10 min at 4°C and the supernatant was filtered through cheesecloth and centrifuged at 8000 g for 10 min at 4°C. The light mitochondrial layer on top of the pellet was removed, and the remaining pellet was resuspended in MSHE, centrifuged again at 8000 g for 10 min at 4°C, and the final pellet was resuspended in a minimal volume of MSHE. Protein concentration was determined using BCA assay (Thermo Fisher Scientific).

Respiration and glycolysis measurements

Oxygen consumption rate (OCR, a measure of oxidative phosphorylation) and extracellular acidification rate (ECAR, a measure of glycolysis) were measured simultaneously using Seahorse XF96 Analyzer (Agilent) in all cell lines and primary cells. XF base medium without phenol red (Agilent, 103335-100) was used as an assay medium. The constituents of this medium are based on DMEM but there is no sodium bicarbonate, glucose, glutamine, or sodium pyruvate. It contains amino acids and vitamins (folic acid, riboflavin, pantothenate, nicotinamide, pyridoxine, and thiamine). Typically, cells were plated 24 h prior to the assay on Seahorse XF96 well plate (Agilent) at the density of 30-40,000 cells per well with multichannel pipette. Three or more technical replicates were run per group. Cells were kept in regular growth media, under 5% CO_2 at 37°C under a humidified atmosphere. Prior to the assay cells were washed twice with assay medium containing 5 mM HEPES, pH 7.4. ± glucose or other tested compounds (details in each figure) and incubated in 37°C, non-CO_2 incubator for 30-40 minutes. In acute exposure experiments, the same protocol was used but glucose or 2-DG were injected through port A. Mitochondrial stress test was then performed using Seahorse XF96 Analyzer (Agilent) to assess key parameters of mitochondrial function.[26] OCR and ECAR measurements were obtained before and after sequential additions of the ATPase inhibitor oligomycin (1 μM), inner membrane uncoupler carbonyl cyanide 4-(trifluoromethoxy) phenylhydrazone (FCCP) (1 μM) and inhibitors of complex I and III rotenone and antimycin A (rot/AA) (0.5 μM each). All compounds were acquired from Sigma. OCR and ECAR values were exported from Seahorse XF Wave software (Agilent) and the following parameters were calculated using Microsoft Excel: baseline OCR (by subtracting the non-mitochondrial respiratory rate from the baseline respiration, pmol/min), maximal OCR (by subtracting the non-mitochondrial respiratory rate from maximal uncoupled respiration, pmol/min), proton (H+) leak (by subtracting the non-mitochondrial respiratory rate from oligomycin-inhibited respiration, pmol/min), ATP-linked respiration (by subtracting the oligomycin-inhibited respiration from basal respiration, pmol/min) and ECAR (basal ECAR before the addition of the compounds, mpH/min). Seahorse XF Real-Time ATP Rate Assay (Agilent, 103592-100) was used to measure ATP production rates and performed as recommended by the manufacturer. OCR measurements were obtained before and after additions of the ATPase inhibitor oligomycin (1 μM) and inhibitors of complex I and III rotenone and antimycin A (rot/AA) (0.5 μM each). Mitochondrial and glycolytic ATP production rates were calculated using Seahorse XF Real-Time ATP Rate Assay Report Generator (Agilent). Since mouse primary PTEC did not tolerate the absence of exogenous substrates, the assay media was supplemented with 1 mM pyruvate and 2 mM glutamine, and the effect of presence or absence of glucose was studied under these conditions.

In experiments with permeabilized cells, assay was performed in MAS buffer (70 mM sucrose, 220 mM mannitol, 10 mM KH_2PO_4, 5 mM $MgCl_2$, 2 mM HEPES, 1 mM EGTA and 0.2% BSA; pH 7.2). The plasma membrane was selectively permeabilized with 2 nM XF plasma membrane permeabilizer (XF PMP, Agilent Technologies) and 0.5 mM pyruvate with 0.5 mM malate were used as substrates along with 4 mM ADP. Mix of 0.5 μM rotenone and 0.5 μM antimycin A (rot/AA) was injected at the end of the experiment and all rates were corrected for background by subtracting the OCR insensitive to rot/AA.

Isolated kidney cortex mitochondria were measured as previously described.[25] Mitochondria were diluted in cold MAS buffer and 5 μg of mitochondria per well was seeded in 20 μl of MAS buffer while keeping the plate on ice. To adhere mitochondria to the bottom of the wells the plate was centrifuged at 2000 g for 20 minutes at 4°C in a centrifuge equipped with a swinging bucket microplate adaptor. The MAS buffer was added to each well to the total volume of 180 μl and the plate was placed in 37°C non-CO_2 incubator for 5 minutes to allow to warm. Phosphorylating respiration (State 3) was measured in the presence of 0.5 mM pyruvate, 0.5 mM malate, and 4 mM ADP. Mix of 0.5 μM rotenone and 0.5 μM antimycin A (rot/AA) was injected at the end of the experiment and all rates were corrected for background by subtracting the OCR insensitive to rot/AA.

Glycolytic intermediates quantification by mass spectrometry

HK-2 cells were plated on 6-well plates (500k per well) in the standard growth media and after 24 h switched to assay media supplemented with no glucose, 5.5 or 25 mM glucose. After 1h, cells were washed in ice-cold PBS, harvested, centrifuged at 200 g for 5 min, and the cell pellet was frozen at -80°C. Modified MPLEx method[27] was used for sample extraction. Briefly, 200 μL of cold methanol was added to the cells and cells were scraped. The resulting homogenate was sonicated on ice for 10 sec. 400 μL of chloroform were added to the homogenate. Then 200 μL of LC-MS grade water with $_{13}C$ internal standards for quantification was added. Samples were centrifuged at 17,000 x g for 10 min and the resulting top layer was collected and taken to dryness under nitrogen. Kidney cortex samples of approximately 20 - 30 mg were received from 6 months old C57BL/6J (WT) mice (The Jackson Laboratory, 000664, RRID:IMSR_JAX:000664) and 5 months old BKS.Cg-Dock7^{m}+/+ Lepr^{db}/J (db/db) mice (The Jackson Laboratory, 000642, RRID:IMSR_JAX:000642). Tissues were homogenized in 200 μL ice-cold methanol with a plastic pestle hand-held homogenizer. Sample was sonicated for 20 s while on ice. 200 μL of water containing internal standards and 400 μL of chloroform were added to the sonicated homogenate. Samples were vortexed briefly and left on ice for 5 min before centrifugation at 15,000 x g for 10 min. The resulting upper layer was collected and dried under nitrogen. Protein quantitation was performed on the resulting protein layer from the sample preparation. All samples were reconstituted in 30 μL of 2:1 ACN: water, filtered, and 5 μL was injected for analysis. Authentic standards with internal standards were also processed and run with the sample queue to generate calibration curves for each metabolite. Compounds were separated on an InfinityLab Poroshell120 HILIC-Z, 2.7 μm, 2.1 × 150 mm column (Agilent Technologies, Memphis, TN, USA) as previously described[28]; the mobile phase A was composed of 90% 10 mM ammonium acetate (pH 9.0) with ammonia and 10% acetonitrile with 2.5 uM InfinityLab Deactivator Additive (Agilent Technologies, Memphis, TN, USA); The mobile phase B was composed of 15% 10 mM ammonium acetate (pH 9.0) with ammonia and 85% acetonitrile with 2.5 uM InfinityLab Deactivator Additive. The flow rate was determined at 0.25 mL/min. The gradient was as follows: 0–2 min at 95% B, 2–5 min at 95% B, 5–5.5 min at 86%, 5.5–8.5 min at 86% B, 8.5–9 min at 84% B, 9–14 min at 84% B, 14–17 min at 80% B, 17–23 min at 60% B, 23–26 min at 60% B, 26–27 min at 95% B, and 27–35 min at 95% B. The temperature of the column compartment was maintained at 25 °C. Metabolites were analyzed on the Agilent 6456 quadrupole time-of-flight (Q-TOF) mass spectrometer coupled to Agilent 1290 LC (Agilent). Data was collected in negative mode, with gas temp at 225 °C, drying gas at 10 L/min, nebulizer at 40 psi, sheath gas temp 300 °C, and sheath gas flow at 12 L/min. Fragmentor was set at 125 V, skimmer at 65 V, and VCap at 3000 V. Metabolomics data was analyzed with Mass Hunter Q-TOF Quantitative Analysis version B.07.01 (Agilent).

QUANTIFICATION AND STATISTICAL ANALYSIS

Statistical analyses were performed using Prism 9.0 (GraphPad). Significance levels were calculated using Student's t test or one-way ANOVA followed by Dunnett's post-hoc test for multiple comparisons. All results from cell culture experiments in the main figures represent at least 3 independent experiments and are expressed as mean ± SEM. Results from cell culture experiments in supplemental figures show representative experiment and are expressed as mean ± SD. P values less than 0.05 were considered statistically significant. Throughout all figures: *$p < 0.05$, **$p < 0.01$, ***$p < 0.001$, and ****$p < 0.0001$.